

Determination of $|V_{us}|$ from a lattice-QCD calculation of the $K \rightarrow \pi \ell \nu$ semileptonic form factor with physical quark masses

A. Bazavov,^{1,2} C. Bernard,³ C.M. Bouchard,⁴ C. DeTar,⁵ Daping Du,⁶ A.X. El-Khadra,^{6,7} J. Foley,⁵ E.D. Freeland,⁸ E. Gámiz,^{9,*} Steven Gottlieb,¹⁰ U.M. Heller,¹¹ Jongjeong Kim,¹² A.S. Kronfeld,⁷ J. Laiho,^{13,14} L. Levkova,⁵ P.B. Mackenzie,⁷ E.T. Neil,^{7,15,16} M.B. Oktay,⁵ Si-Wei Qiu,⁵ J.N. Simone,⁷ R. Sugar,¹⁷ D. Toussaint,¹² R.S. Van de Water,⁷ and Ran Zhou^{10,7}

(Fermilab Lattice and MILC Collaborations)

¹*Physics Department, Brookhaven National Laboratory, Upton, New York, USA*

²*Department of Physics and Astronomy, University of Iowa, Iowa, USA*

³*Department of Physics, Washington University, St. Louis, Missouri, USA*

⁴*Department of Physics, The Ohio State University, Columbus, Ohio, USA*

⁵*Physics Department, University of Utah, Salt Lake City, Utah, USA*

⁶*Physics Department, University of Illinois, Urbana, Illinois, USA*

⁷*Fermi National Accelerator Laboratory, Batavia, Illinois, USA*

⁸*Liberal Arts Department, School of the Art Institute of Chicago, Chicago, Illinois, USA*

⁹*CAFPE and Departamento de Física Teórica y del Cosmos, Universidad de Granada, Granada, Spain*

¹⁰*Department of Physics, Indiana University, Bloomington, Indiana, USA*

¹¹*American Physical Society, Ridge, New York, USA*

¹²*Department of Physics, University of Arizona, Tucson, Arizona, USA*

¹³*SUPA, School of Physics and Astronomy, University of Glasgow, Glasgow, UK*

¹⁴*Department of Physics, Syracuse University, Syracuse, New York, USA*

¹⁵*Department of Physics, University of Colorado, Boulder, Colorado, USA*

¹⁶*RIKEN-BNL Research Center, Brookhaven National Laboratory, Upton, New York, USA*

¹⁷*Department of Physics, University of California, Santa Barbara, California, USA*

(Dated: December 5, 2013)

We calculate the kaon semileptonic form factor $f_+(0)$ from lattice QCD, working, for the first time, at the physical light-quark masses. We use gauge configurations generated by the MILC collaboration with $N_f = 2 + 1 + 1$ flavors of sea quarks, which incorporate the effects of dynamical charm quarks as well as those of up, down, and strange. We employ data at three lattice spacings to extrapolate to the continuum limit. Our result, $f_+(0) = 0.9704(32)$, where the error is the total statistical plus systematic uncertainty added in quadrature, is the most precise determination to date. Combining our result with the latest experimental measurements of K semileptonic decays, one obtains the Cabibbo-Kobayashi-Maskawa matrix element $|V_{us}| = 0.22290(74)(52)$, where the first error is from $f_+(0)$ and the second one is from experiment. In the first-row test of Cabibbo-Kobayashi-Maskawa unitarity, the error stemming from $|V_{us}|$ is now comparable to that from $|V_{ud}|$.

PACS numbers: 13.20.Eb, 12.15.Hh, 12.38.Gc

Introduction: The Cabibbo-Kobayashi-Maskawa [1] (CKM) matrix underpins all quark flavor-changing interactions in the standard model of particle physics. Symmetries reduce the number of physical parameters of this 3×3 unitary matrix to four. They can be taken to be $|V_{us}|$, $|V_{ub}|$, $|V_{cb}|$, and $\arg(V_{ub}^*)$, where subscripts denote the quark flavors interacting with the W boson. The focus of this Letter is to reduce the theoretical uncertainty in the first of these, in a way that sharpens the test of CKM unitarity from the first row of the matrix.

The test asks whether, or how precisely,

$$\Delta_u \equiv |V_{ud}|^2 + |V_{us}|^2 + |V_{ub}|^2 - 1 \quad (1)$$

vanishes. The CKM matrix elements are determined from, respectively, superallowed nuclear β decays, kaon decays, and B -meson decays to charmless final states. A failure of the test would be evidence for phenomena beyond the standard model, for example further generations of quarks and leptons, beyond those observed, or nonstandard amplitudes contributing to the decays. As it happens, Δ_u and analogous tests remain in agreement with the CKM paradigm. Still, the absence of deviations provides stringent constraints on nonstandard phenomena and the energy scale at which they may occur [2].

Until now, the error

$$\begin{aligned} \delta\Delta_u^2 = & 4|V_{ud}|^2 (\delta|V_{ud}|)^2 + 4|V_{us}|^2 (\delta|V_{us}|)^2 \\ & + 4|V_{ub}|^2 (\delta|V_{ub}|)^2 \end{aligned} \quad (2)$$

has been dominated by the second term, because $|V_{ud}| = 0.97425 \pm 0.00022$ is so precise [3] (the third term is negligible). One can determine $|V_{us}|$ via the axial-vector current, i.e., leptonic kaon decays [4–10], or via the vector current, i.e., semileptonic decays [11–15]. The current precision is at the level of 0.23–0.4% [9, 10] for the former, but only $\sim 0.5\%$ [14, 15], for the latter. According to the standard model, both approaches should yield the same result, because the W -boson current has the structure $V - A$.

For semileptonic decays, the relation between the experimentally measured $K \rightarrow \pi l \nu(\gamma)$ inclusive decay width and the CKM matrix element $|V_{us}|$, up to well known overall factors, is [16]

$$\Gamma_{K_{l3}(\gamma)} \propto |V_{us}|^2 \left| f_+^{K^0 \pi^-}(0) \right|^2 \left(1 + \delta_{\text{EM}}^{Kl} + \delta_{\text{SU}(2)}^{K\pi} \right). \quad (3)$$

The quantities δ_{EM}^{Kl} and $\delta_{\text{SU}(2)}^{K\pi}$ denote long-distance electromagnetic and strong isospin-breaking corrections, respectively [16]. The latter is defined as a correction relative to the K^0 mode. The quantity needed from lattice QCD is the vector form factor $f_+(0)$, defined by

$$\begin{aligned} \langle \pi(p_\pi) | V^\mu | K(p_K) \rangle = & f_+^{K\pi}(q^2) \left[p_K^\mu + p_\pi^\mu - \frac{m_K^2 - m_\pi^2}{q^2} q^\mu \right] \\ & + f_0^{K\pi}(q^2) \frac{m_K^2 - m_\pi^2}{q^2} q^\mu, \end{aligned} \quad (4)$$

where $V^\mu = \bar{s}\gamma^\mu u$ is the appropriate flavor-changing vector current, and $q = p_K - p_\pi$ is the momentum transfer.

We previously [14] presented a lattice-QCD calculation of $f_+(0)$ using the $N_f = 2 + 1$ gauge-field configurations generated by the MILC Collaboration. The RBC/UKQCD Collaboration presented an independent calculation [15], using a different set of $N_f = 2 + 1$ gauge-field configurations. Even though in both works the error on $|V_{us}|$ from $f_+(0)$ is reduced to $\sim 0.5\%$, it is still roughly a factor of two larger than the experimental uncertainty from $\Gamma_{K_{l3}(\gamma)}$. Therefore, further improvement is necessary, and we take an important step in this Letter.

Before, our dominant systematic uncertainty came from the chiral extrapolation of light-quark masses from their simulation values to the physical point [14]. Here, we reduce this uncertainty with data directly at the physical light-quark mass. Thus, the extrapolation becomes an interpolation. We work with a subset of the $N_f = 2 + 1 + 1$ ensembles generated (again) by the MILC Collaboration [17]. The new ensembles use an action for the sea quarks with three-times smaller discretization effects. We now use three different lattice spacings, instead of only two, to control these and other discretization effects. In these ensembles, the strange sea-quark masses are much better tuned than before, reducing another important uncertainty in Ref. [14]. Finally, the new ensembles include the effects of charm quarks in the sea.

Simulation details and statistical errors: We largely follow the strategy of Ref. [14]. Hence, this Letter only summarizes the main features and points out the differences. We refer the reader to Ref. [14] for details of our methodology and to Ref. [18] for technical details of the current numerical work.

We obtain the needed form factor using the relation

$$f_+(0) = f_0(0) = \frac{m_s - m_l}{m_K^2 - m_\pi^2} \langle \pi(p_\pi) | S | K(p_K) \rangle, \quad (5)$$

where $S \equiv \bar{s}u$. The last expression requires no renormalization and allows us to extract the form factor from three-point correlation functions with insertion of a scalar current instead of a noisier vector current [19]. The momentum of the pion, p_π , is adjusted via partially twisted boundary conditions [20, 21], such that $q^2 = 0$. Unlike in Ref. [14], we do not consider correlation functions with nonzero kaon momentum, because they end up being noisier.

Table I shows the simulation parameters of the ensembles used here [17]. These ensembles use a one-loop Symanzik-improved gauge action for the gluons [22, 23], and the highly-improved staggered-quark (HISQ) action [24] for the u , d , s , and c quarks in the sea. The HISQ sea quarks were simulated with the fourth-root procedure for eliminating extra quark species (often known as tastes) arising from fermion doubling [25–34].

We study data at four different values of the lattice spacing. The number of configurations analyzed at

TABLE I. Parameters of the $N_f = 2 + 1 + 1$ gauge-field ensembles used in this work and details of the correlation functions generated. N_{conf} is the number of configurations included in our analysis, N_{src} the number of time sources used on each configuration, and L the spatial size of the lattice. Pion masses (fourth and fifth columns) are given in MeV. Further information about the ensembles, including the light and charm quark masses, can be found in Ref. [17].

$\approx a$ (fm)	am_s^{sea}	am_s^{val}	m_π^P	m_π^{RMS}	$m_\pi L$	N_{conf}	N_{src}
0.15	0.0647	0.06905	133	311	3.30	1000	4
0.12	0.0509	0.0535	309	370	4.54	1053	8
	0.0507	0.053	215	294	4.29	993	4
	0.0507	0.053	215	294	5.36	391	4
	0.0507	0.0531	133	241	3.88	945	8
0.09	0.037	0.038	312	332	4.50	775	4
	0.0363	0.038	215	244	4.71	853	4
	0.0363	0.0363	128	173	3.66	621	4
0.06	0.024	0.024	319	323	4.51	362	4

$a \approx 0.06$ is too small to remove autocorrelation effects in a controlled way, so this data set is not used in the central fit but as a cross-check of discretization effects. The three lattice spacings included in our main analysis, $a \approx 0.15, 0.12, 0.09$ fm, allow us to perform a well-controlled extrapolation to continuum QCD.

The strange and charmed masses are always near their physical values. In most cases, however, a better tuning of m_s became available before computing the matrix element in Eq. (5). We have chosen the better tuned value for the valence quarks, hence the different values of m_s^{val} and m_s^{sea} in the second and third columns. The up and down sea-quark masses are taken to be the same: $m_l = 0.2m_s, 0.1m_s, \text{ or } m_s/27$. The last corresponds very nearly to the physical pion mass: compare the entries in the fourth column of Table I with the physical pion mass, 135 MeV. We include data at heavier-than-physical pion masses on the $a \approx 0.12$ and 0.09 fm ensembles to further control the chiral-continuum fit.

While the column labeled by m_π^P in Table I corresponds to the valence pion, the root-mean-squared pion mass, m_π^{RMS} , provides a measure of the dominant discretization effects, due to lattice-artifact interactions between staggered quarks of different tastes. These taste splittings, are of order $\alpha_s^2 a^2$ for the HISQ action, where α_s is the strong coupling at a scale around π/a . They decrease rapidly with the lattice spacing, as can be seen from the difference of the fifth and fourth columns in Table I.

We obtain both hadronic matrix elements and meson masses and energies from combined fits of two-point and three-point correlation functions. The general structure of these three-point functions is depicted in Fig. 1. The correlation function fits include the ground states as well as excited and opposite-parity states [14]. To remove excited-state contamination, we fit three-point functions with both even and odd source-sink separation, denoted T in Fig. 1.

Autocorrelations between configurations make it necessary to block the data to obtain accurate statistical errors. By examining the fit parameters' error estimates, we find that blocking by four accounts sufficiently for the autocorrelation. We thus block all data included in the main analysis by four.

Our correlation-function fits are stable under variations of the number of states, time ranges, source-sink separations, and other aspects of the fits. The central values and statistical errors are shown as a function of the light quark mass in Fig. 2, which is discussed in more detail below. Numerical values are given in Ref. [18]. Within the statistical errors of relative size $\sim 0.2\text{--}0.4\%$, the data show no discretization effects except possibly at 0.15 fm, as expected with the HISQ action.

Chiral interpolation and continuum extrapolation: Even though we have data at the physical quark masses, we include data at larger m_π , for several reasons. First, the use of chiral perturbation theory (χ PT) and data at different masses allows us to correct for small mistunings of the light- and strange-quark masses, as well as for partially quenched effects due to $m_s^{\text{val}} \neq m_s^{\text{sea}}$. In addition, these data are very precise, so including them in the chiral interpolation helps to reduce the final statistical error, especially since our physical-mass data set at $a \approx 0.09$ fm has lower statistics than the other ensembles. Furthermore, the dominant discretization effects, which stem from the extra tastes of staggered fermions, are well-described by the χ PT formula [35, 36], so they are removed when taking the continuum limit.

In χ PT, the form factor $f_+(0)$ can be written as $f_+(0) = 1 + f_2 + f_4 + \dots$. In continuum QCD, the Ademollo-Gatto theorem [37] ensures that the $\mathcal{O}(p^{2i})$ chiral corrections f_{2i} tend to zero in the SU(3) limit as $(m_K^2 - m_\pi^2)^2$. In particular, f_2 is completely fixed in terms of well-known quantities. At finite lattice spacing, however, violations of the Ademollo-Gatto theorem arise from discretization effects in the dispersion relation needed to derive the relation in Eq. (5).

We perform the interpolation to the physical masses and the continuum using next-to-next-to-leading-order

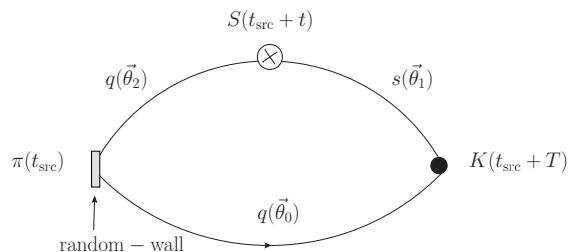


FIG. 1. Structure of the three-point correlation functions. Light-quark propagators are generated at t_{src} with random-wall sources and propagate to $T + t_{\text{src}}$, where an extended strange propagator starts. The twist angles $\vec{\theta}_2$ yields $\vec{p}_\pi = \vec{\theta}_2 \pi/L$, and in this work $\vec{\theta}_0 = \vec{\theta}_1 = 0$.

(NNLO) continuum χ PT [38], supplemented by next-to-leading-order (NLO) partially quenched, staggered χ PT [39]. Because we observe almost no lattice-spacing dependence in our data, discretization effects in higher-loop χ PT should be negligible. After removing the dominant discretization effects with S χ PT, the remaining ones, which stem from violations of the continuum dispersion relation and higher orders taste-splitting effects, are of order $\alpha_s a^2$, a^4 , $(m_K^2 - m_\pi^2)^2 \alpha_s a^2$, and $(m_K^2 - m_\pi^2)^2 \alpha_s^2 a^2$. We therefore introduce fit parameters for these terms— K_1 , K_3 , K_2 , and K'_2 , respectively—and take the functional form

$$f_+(0) = 1 + f_2^{\text{PQS}\chi\text{PT}}(a) + K_1 a^2 \sqrt{\bar{\Delta}} + K_3 a^4 + f_4^{\text{cont}} + (m_\pi^2 - m_K^2)^2 \left[C_6 + K_2 a^2 \sqrt{\bar{\Delta}} + K'_2 a^2 \bar{\Delta} + C_8 m_\pi^2 + C_{10} m_\pi^4 \right], \quad (6)$$

where $f_2^{\text{PQS}\chi\text{PT}}(a)$ is the NLO partially quenched staggered χ PT expression with the leading isospin corrections added [40], f_4^{cont} is the sum of the NNLO continuum chiral logarithms, and $a^2 \bar{\Delta}$ is the average taste splitting, with $\bar{\Delta}$ used as a proxy for α_s^2 . The analytic term C_6 is related to a combination of low-energy constants in continuum χ PT, and C_8 and C_{10} are fit parameters that parametrize chiral corrections at N³LO and N⁴LO, respectively. We take the taste splittings from Ref. [17] and set the rest of the inputs in the same way as in Ref. [14]. The fit parameters are constrained with Bayesian techniques and determined in the chiral fit. We fix their prior widths using power counting arguments,

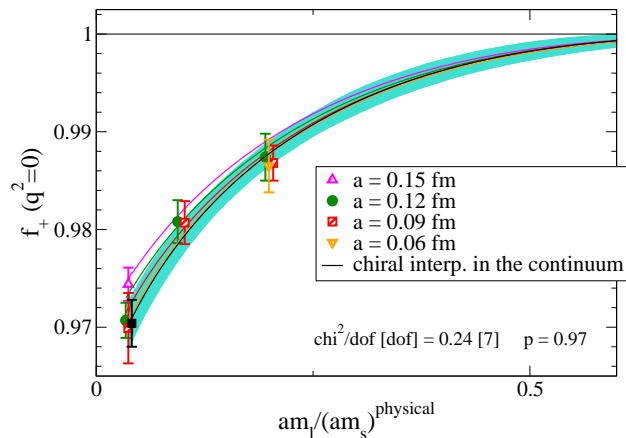


FIG. 2. Form factor $f_+(0)$ vs. light-quark mass. Errors shown are statistical only, obtained from 500 bootstraps. Different symbols and colors denote different lattice spacings, and the corresponding colored lines show the chiral interpolation at fixed lattice spacing. The solid black line is the interpolation in the light-quark mass, keeping m_s equal to its physical value, and turning off all discretization effects. The turquoise error band includes statistical, discretization, and higher order chiral errors, as explained in the text.

TABLE II. Stability of the continuum extrapolation with omission of discretization terms, in the notation of Eq. (6).

Parameters omitted	$f_+(0)$	χ^2/dof	p
$C_8, C_{10}, K_1, K_2, K_3, K'_2$	0.9714(12)	0.27	0.97
$C_8, C_{10}, K_1, K_2, K_3$	0.9703(23)	0.24	0.97
C_8, C_{10}, K_2, K_3	0.9703(23)	0.24	0.97
C_8, C_{10}, K_3	0.9703(23)	0.24	0.97
C_8, C_{10}	0.9703(23)	0.24	0.97
Central fit: full Eq. (6)	0.9704(24)	0.24	0.97

except for K'_2 , where we conservatively triple the power-counting width, since it is the numerically dominant term in our fits [18]. Using Eq. (6) expressed in terms of meson masses, we interpolate to physical pion and kaon masses with electromagnetic effects removed [41, 42]: $m_{\pi^+}^{\text{QCD}} = 135.0$ MeV, $m_{K^0}^{\text{QCD}} \approx m_{K^0}^{\text{phys}} = 497.7$ MeV, and $m_{K^+}^{\text{QCD}} = 491.6$ MeV. The last value enters only in f_2 , since the isospin-conserving result is used at NNLO.

We estimate the statistical errors by generating a set of 500 pseudo-ensembles via the bootstrap method, and repeating the fit on each pseudo-ensemble. The result from the chiral and continuum interpolation/extrapolation is $f_+(0) = 0.9704(24)$, which is shown in Fig. 2 together with the data points. The fits cannot precisely determine the coefficients K_i in Eq. (6), since only the $a \approx 0.15$ fm point appears to show any discretization effects. We examine this issue further by performing fits with fewer parameters, including one by one the analytical a^2 terms in Eq. (6), and excluding higher order chiral terms (third line in Eq. (6)) to make the comparison cleaner. The results of these fits are shown in Table II. We find no difference except when all of the discretization effects are omitted. Something similar happens with the addition of higher order chiral terms to the fit function. Adding a N³LO term slightly changes the central value and increases the error from 0.9703(23) to 0.9704(24). Adding a N⁴LO term does not change either the central value or the error. The alternate fits with additional discretization terms and/or chiral terms show that fit errors are saturated. We thus consider the error from the chiral and continuum interpolation/extrapolation with the fit function in Eq. (6), $f_+(0) = 0.9704(24)$, as the total statistical+discretization+chiral interpolation error. We discuss further tests of the robustness of this Bayesian error estimate strategy in Ref. [18].

Although we do not include it in the chiral and continuum interpolation/extrapolation because of low statistics, we also show data on an ensemble with a smaller lattice spacing, $a \approx 0.06$ fm, and $m_l^{\text{sea}} = 0.2m_s^{\text{sea}}$, an (orange) down-pointing triangle in Fig. 2. It lies on top of the results for the other lattice spacings, confirming that discretization effects are already much smaller than statistical errors. We can infer the same conclusion from the fact that the red line in Fig. 2, which corresponds to

$a \approx 0.09$ fm, is very close to the continuum one. The remaining sources of systematic uncertainty that make significant contributions to the total error are given in Table III. We estimate the error due to including partially quenched effects only at one loop by the shift in the final result when using m_s^{val} or m_s^{sea} in the NNLO chiral logarithmic function, f_4^{cont} . To convert dimensionful quantities from lattice to physical units, we use the scale $r_1 = 0.3117(22)$ fm [43] obtained from the static-quark potential [44, 45]. The form factor, being a dimensionless quantity, depends on the scale only via the input parameters. Propagating the uncertainty in the scale through to $f_+(0)$ yields the entry shown in Table III. For an estimate of the finite volume error we compare our data obtained with two different spatial volumes and other parameters at $a \approx 0.12$ fm fixed. The difference is about half of the statistical error, so we conservatively take the finite volume error to be the full size of the statistical error. Finally, we estimate the error from the NNLO and higher order isospin corrections to the $K^0\pi^+$ mode by taking twice the difference between the NNLO contribution to $f_+(0)$ with and without isospin corrections [46]. A more detailed discussion of all errors and tests performed is given in Ref. [18].

Final result and conclusions: Our final result for the vector form factor is

$$f_+(0) = 0.9704(24)(22) = 0.9704(32), \quad (7)$$

where the first error is from the chiral-continuum fit, and the second the sum in quadrature of the other systematic errors listed in Table III. This result is the most precise calculation of $f_+(0)$ to date and the first to include data at physical light-quark masses. It agrees with the previous results of Refs. [14, 15], with a reduced total uncertainty of 0.33%.

Using the latest average of experimental results for K semileptonic decays, $|V_{us}|f_+(0) = 0.2163(5)$ [47], and the form factor in Eq. (7), one obtains

$$|V_{us}| = 0.22290(74)_{f_+(0)}(52)_{\text{expt}} = 0.22290(90). \quad (8)$$

The unitarity test becomes

$$\Delta_u = -0.00115(40)_{V_{us}}(43)_{V_{ud}}, \quad (9)$$

i.e., the error on Δ_u from $|V_{us}|$ is now slightly smaller than that from $|V_{ud}|$. Combining the two errors, one sees a $\sim 2\sigma$ tension with unitarity. Recall that the semileptonic decay proceeds through the vector current; the uncertainty of $|V_{us}|/|V_{ud}|$ from the axial-vector current, via leptonic pion and kaon decays and the ratio f_K/f_π [10] already results in a value of Δ_u with smaller error. As emphasized above, it is important to carry out the test with both currents.

In summary, with the HISQ, $N_f = 2 + 1 + 1$ ensembles, we have reduced the uncertainties on $|V_{us}|$ from the chiral interpolation and discretization effects. The main

TABLE III. Error budget for $f_+(0)$ in percent.

Source of uncertainty	Error $f_+(0)$ (%)
Statistics + discretization + chiral interpolation	0.24
$m_s^{\text{val}} \neq m_s^{\text{sea}}$	0.03
Scale r_1	0.08
Finite volume	0.2
Isospin	0.016
Total Error	0.33

remaining sources of error are Monte Carlo statistics and finite-volume effects. In order to reach the final target of 0.2% precision required by experiment, we are increasing statistics and deriving the finite-volume corrections at one-loop in partially quenched staggered χ PT with twisted boundary conditions [48].

Acknowledgements: We thank Christine Davies for useful discussions. We thank Johan Bijmans for making his NLO partially quenched χ PT and NNLO full QCD χ PT codes available to us. A.X.K. thanks the Fermilab theory group for hospitality while this work was finalized. Computations for this work were carried out with resources provided by the USQCD Collaboration, the Argonne Leadership Computing Facility and the National Energy Research Scientific Computing Center, which are funded by the Office of Science of the United States Department of Energy; and with resources provided by the National Center for Atmospheric Research, the National Center for Supercomputing Applications, the National Institute for Computational Science, and the Texas Advanced Computing Center, which are funded through the National Science Foundation's Teragrid/XSEDE and Blue Waters Programs. This work was supported in part by the U.S. Department of Energy under Grants No. DE-FG02-91ER40628 (C.B.), No. DE-FC02-06ER41446 (C.D., J.F., L.L., M.B.O.), No. DE-FG02-91ER40661 (S.G., R.Z.), No. DOE DE-FG02-13ER42001 (D.D., A.X.K.), No. DE-FG02-04ER-41298 (J.K., D.T.); by the National Science Foundation under Grants No. PHY-1067881, No. PHY-0757333, No. PHY-0703296 (C.D., J.F., L.L., M.B.O.), No. PHY-0757035 (R.S.); by the URA Visiting Scholars' program (A.X.K.); by the Science and Technology Facilities Council and the Scottish Universities Physics Alliance (J.L.); by the MINECO (Spain) under Grants FPA2010-16696, FPA2006-05294, and *Ramón y Cajal* program (E.G.); by Junta de Andalucía (Spain) under Grants FQM-101 and FQM-6552 (E.G.); and by European Commission under Grant No. PCIG10-GA-2011-303781 (E.G.). This manuscript has been co-authored by an employee of Brookhaven Science Associates, LLC, under Contract No. DE-AC02-98CH10886 with the U.S. Department of Energy. Fermilab is operated by Fermi Research Alliance, LLC, under Contract No. DE-AC02-07CH11359 with the U.S. Department of Energy.

* megamiz@ugr.es

- [1] N. Cabibbo, Phys. Rev. Lett. **10**, 531 (1963); M. Kobayashi and T. Maskawa, Prog. Theor. Phys. **49**, 652 (1973).
- [2] V. Cirigliano, J. Jenkins and M. González-Alonso, Nucl. Phys. B **830** (2010) 95 [arXiv:0908.1754 [hep-ph]].
- [3] J. C. Hardy and I. S. Towner, Phys. Rev. C **79**, 055502 (2009) [arXiv:0812.1202 [nucl-ex]].
- [4] E. Follana *et al.* [HPQCD and UKQCD Collaborations], Phys. Rev. Lett. **100**, 062002 (2008) [arXiv:0706.1726 [hep-lat]].
- [5] S. Dürr *et al.*, Phys. Rev. D **81**, 054507 (2010) [arXiv:1001.4692 [hep-lat]].
- [6] Y. Aoki *et al.* [RBC and UKQCD Collaborations], Phys. Rev. D **83**, 074508 (2011) [arXiv:1011.0892 [hep-lat]].
- [7] A. Bazavov *et al.* [MILC Collaboration], PoS **LATTICE2010**, 074 (2010) [arXiv:1012.0868 [hep-lat]].
- [8] J. Laiho and R. S. Van de Water, PoS **LATTICE2011**, 293 (2011) [arXiv:1112.4861 [hep-lat]].
- [9] A. Bazavov *et al.* [MILC Collaboration], Phys. Rev. Lett. **110**, 172003 (2013) [arXiv:1301.5855 [hep-ph]].
- [10] R. J. Dowdall, C. T. H. Davies, G. P. Lepage and C. McNeile [HPQCD Collaboration], Phys. Rev. D **88**, 074504 (2013) [arXiv:1303.1670 [hep-lat]].
- [11] V. Lubicz *et al.* [ETM Collaboration], Phys. Rev. D **80** (2009) 111502 [arXiv:0906.4728 [hep-lat]].
- [12] P. A. Boyle *et al.* [RBC/UKQCD Collaboration], Eur. Phys. J. C **69** (2010) 159 [arXiv:1004.0886 [hep-lat]].
- [13] T. Kaneko *et al.* [JLQCD Collaboration], PoS **LATTICE2012**, 111 (2012) [arXiv:1211.6180 [hep-lat]].
- [14] A. Bazavov *et al.* [Fermilab Lattice and MILC Collaborations], Phys. Rev. D **87**, 073012 (2013) [arXiv:1212.4993 [hep-lat]].
- [15] P. A. Boyle, J. M. Flynn, N. Garron, A. Jüttner, C. T. Sachrajda, K. Sivalingam, and J. M. Zanotti [RBC/UKQCD Collaboration], JHEP **1308**, 132 (2013) [arXiv:1305.7217 [hep-lat]].
- [16] V. Cirigliano, G. Ecker, H. Neufeld, A. Pich and J. Portolés, Rev. Mod. Phys. **84**, 399 (2012) [arXiv:1107.6001 [hep-ph]].
- [17] A. Bazavov *et al.* [MILC Collaboration], Phys. Rev. D **82**, 074501 (2010) [arXiv:1004.0342 [hep-lat]]; A. Bazavov *et al.* [MILC Collaboration], Phys. Rev. D **87**, 054505 (2013) [arXiv:1212.4768 [hep-lat]].
- [18] E. Gámiz *et al.* [Fermilab Lattice and MILC Collaborations], PoS **LATTICE2013**, 395 (2013) [arXiv:1311.7264 [hep-lat]].
- [19] H. Na, C. T. H. Davies, E. Follana, G. P. Lepage, J. Shigemitsu [HPQCD Collaboration], Phys. Rev. D **82** (2010) 114506 [arXiv:1008.4562 [hep-lat]].
- [20] P. F. Bedaque, J.-W. Chen, Phys. Lett. B **616**, 208-214 (2005) [hep-lat/0412023].
- [21] C. T. Sachrajda and G. Villadoro, Phys. Lett. B **609**, 73 (2005) [hep-lat/0411033].
- [22] M. Lüscher and P. Weisz, Phys. Lett. B **158**, 250 (1985).
- [23] A. Hart *et al.* [HPQCD Collaboration], Phys. Rev. D **79**, 074008 (2009) [arXiv:0812.0503 [hep-lat]].
- [24] E. Follana *et al.* [HPQCD and UKQCD Collaborations], Phys. Rev. D **75**, 054502 (2007) [hep-lat/0610092].
- [25] E. Marinari, G. Parisi and C. Rebbi, Nucl. Phys. B **190**, 734 (1981).
- [26] S. Dürr and C. Hoelbling, Phys. Rev. D **69**, 034503 (2004) [hep-lat/0311002].
- [27] E. Follana, A. Hart and C.T.H. Davies [HPQCD and UKQCD Collaborations], Phys. Rev. Lett. **93** (2004) 241601 [hep-lat/0406010].
- [28] S. Dürr, C. Hoelbling and U. Wenger, Phys. Rev. D **70**, 094502 (2004) [hep-lat/0406027].
- [29] Y. Shamir, Phys. Rev. D **71**, 034509 (2005) [hep-lat/0412014]; Phys. Rev. D **75**, 054503 (2007) [hep-lat/0607007].
- [30] C. Bernard, Phys. Rev. D **73**, 114503 (2006) [hep-lat/0603011].
- [31] C. Bernard, M. Golterman, Y. Shamir and S. R. Sharpe, Phys. Lett. B **649**, 235 (2007) [hep-lat/0603027].
- [32] C. Bernard, M. Golterman and Y. Shamir, Phys. Rev. D **77**, 074505 (2008) [arXiv:0712.2560 [hep-lat]].
- [33] D. H. Adams, Phys. Rev. D **77**, 105024 (2008) [arXiv:0802.3029 [hep-lat]].
- [34] G. C. Donald, C. T. H. Davies, E. Follana and A. S. Kronfeld, Phys. Rev. D **84**, 054504 (2011) [arXiv:1106.2412 [hep-lat]].
- [35] W.-J. Lee and S. R. Sharpe, Phys. Rev. D **60**, 114503 (1999) [hep-lat/9905023].
- [36] C. Aubin and C. Bernard, Phys. Rev. D **68**, 034014 (2003) [arXiv:hep-lat/0304014]; Phys. Rev. D **68**, 074011 (2003) [arXiv:hep-lat/0306026].
- [37] M. Ademollo and R. Gatto, Phys. Rev. Lett. **13**, 264 (1964).
- [38] J. Bijnens and P. Talavera, Nucl. Phys. B **669**, 341 (2003) [hep-ph/0303103].
- [39] C. Bernard, J. Bijnens and E. Gámiz, arXiv:1311.7511 [hep-lat].
- [40] J. Gasser and H. Leutwyler, Nucl. Phys. B **250**, 517 (1985).
- [41] S. Aoki *et al.* [FLAG Working Group], arXiv:1310.8555 [hep-lat].
- [42] S. Basak *et al.* [MILC Collaboration], PoS **CD12**, 030 (2013) [arXiv:1301.7137 [hep-lat]].
- [43] A. Bazavov *et al.* [Fermilab Lattice and MILC Collaborations], Phys. Rev. D **85**, 114506 (2012) [arXiv:1112.3051 [hep-lat]].
- [44] C. W. Bernard *et al.*, Phys. Rev. D **62**, 034503 (2000) [hep-lat/0002028].
- [45] R. Sommer, Nucl. Phys. B **411**, 839 (1994) [hep-lat/9310022].
- [46] J. Bijnens and K. Ghorbani, arXiv:0711.0148 [hep-ph].
- [47] M. Moulson, "Testing the Standard Model with Kaon Decays," in *CIPANP 2012*, edited by B. Fleming (AIP, Melville, NY, 2013) [arXiv:1209.3426 [hep-ex]].
- [48] C. Bernard, J. Bijnens and E. Gámiz, in preparation.